

Feathery grain growth during solidification under forced flow conditions

A.N. Turchin^{a,*}, M. Zuijderwijk^b, J. Pool^b, D.G. Eskin^a, L. Katgerman^c

^a Netherlands Institute for Metals Research, Mekelweg 2, 2628CD Delft, The Netherlands

^b Corus Research, Development and Technology, 1970CA IJmuiden, The Netherlands

^c Delft University of Technology, Mekelweg 2, 2628CD Delft, The Netherlands

Received 18 December 2006; received in revised form 21 February 2007; accepted 22 February 2007

Available online 5 April 2007

Abstract

The grain morphology developed during solidification of an Al–4.5% Cu alloy is represented generally by columnar or equiaxed dendrites. Twinned feathery grains are found in the structure formed under certain heat and flow conditions during solidification. In this work, these conditions were achieved during solidification in a cavity under forced flow. Feathery grain formation is studied by means of fluid dynamics simulations with solidification included and by experiments. In order to determine the crystallographic orientation of feathery grains, electron backscattered diffraction measurements were performed. The growth features of feathery grains were analyzed by observations made normal and parallel to the growth direction. Some correlations between twinned feathery morphology, flow and solidification parameters were obtained.

© 2007 Acta Materialia Inc. Published by Elsevier Ltd. All rights reserved.

Keywords: Solidification; Aluminium alloys; Twinning

1. Introduction

Casting is one of the most important processes of manufacturing which allows one to obtain a product with a complex geometry and a size covering a wide weight range from grams to a few tons. Furthermore, uniform structure and properties throughout the casting are crucial for the quality of the final product.

The as-cast structures of aluminium alloys developed during industrial processes (direct-chill casting, continuous casting, strip casting, shape casting, etc.) usually consist of columnar and equiaxed grains. After nucleation has occurred, the solid/liquid interface takes on a specific pattern at the atomic scale. Aluminium alloys solidify with a rough interface – which exposes a lot of sides for the attachment of atoms from the liquid – and are non-faceted at the microscopic scale [1]. However, it has been shown that the structure of aluminium alloys can exhibit a grain morphology associated with faceted growth, the so-called

“feathery grain” morphology consisting of large elongated grains of twinned dendrites [2]. Using an anodic oxidation technique and polarized light it is possible to reveal the feathery grains in the as-cast structure of aluminium alloys.

Feathery grains dramatically affect the properties of the solidified structure during casting or welding, impairing the deformability of the material, and render changes to the microstructure via heat treatment impossible [3,4]. Their appearance during solidification processing is believed to be promoted by a high temperature gradient at the solidification front, a high cooling rate [5] and the presence of convection [6] and/or certain alloying elements [7]. Currently, one of the most useful practical approaches applied in casting and welding practice aimed at avoiding feathery growth is the addition of a grain refiner [8].

Several comprehensive studies on feathery grain growth were carried out during the last decade [6,9,10]. Electron backscattered diffraction (EBSD) investigation of the feathery grain texture in unidirectional solidified Al–Cu, Al–Si and Al–Mg, and direct-chill cast Al–Mg–Si alloys shows that feathery grains are made of twinned lamellae with $\langle 111 \rangle$ primary dendrite trunks split in their centers

* Corresponding author. Tel.: +31 152783146.

E-mail address: a.turchin@nimr.nl (A.N. Turchin).

by the coherent $\{111\}$ twin plate. These grains are separated by straight or wavy boundaries. It has been demonstrated that the orientation of the trunks is close to the thermal gradient direction. Secondary dendrite branches also grow along the $\langle 110 \rangle$ direction and their impingement creates wavy non-coherent twin boundaries between the coherent twin planes. Finally, it is suggested that feathery grain morphology appears as a result of two combined mechanisms occurring on the atomic scale. First, it is a change in the anisotropic properties of an alloy (surface tension, atom attachment kinetics), which at a high growth rate switches the preferential growth direction from $\langle 100 \rangle$ to $\langle 110 \rangle$. The second mechanism is the symmetry of the growth directions of the dendrite arms by a twinning operation initialized by stacking faults.

Recently, the influence of convection on the formation of feathery grains was studied in a 1050 alloy obtained during semicontinuous casting in a mold with lateral liquid feeding [6]. Feathery grains were observed in the region opposite to the melt entrance where the change of the velocity field is the highest. Moreover, the grains have their $[011]$ trunks and $[110]$ side arms growing in the direction opposite to the convection currents. Although understanding of the nature, growth habit and ways to avoid feathery growth is quite advanced, the correlations between the solidification parameters and feathery grain formation during solidification are seldom available.

This paper provides results on feathery grain formation during solidification in a cavity under forced flow conditions of an Al–4.5% Cu alloy. The forced flow was created by an electromagnetic pump producing a flow of constant velocity at the required melt temperature.

2. Experimental procedure

A series of samples of an Al–4.5% Cu alloy were solidified in a cavity under conditions of constant forced flow along the solidification front. The experimental technique used has been described in detail elsewhere [11]. The set-up consisted of an electromagnetic pump, process control, melt-guiding and data acquisition systems. A “flow-through” melt-guiding system was designed in this work in order to obtain a constant unidirectional bulk flow along the solidification front with the control of the flow rate. The pump created a linear flow that passed through a rectangular launder with dimensions of $800 \times 60 \times 70$ mm into a crucible. Solidification occurred under conditions of constant melt flow along the solidification front on the bottom side of a water-cooled bronze chill built in the bottom of the launder. The chill had a rectangular shape 34×110 mm in plane section with the inner cavity $\sim 10 \times 100$ mm. A schematic drawing of the structure developed during solidification under forced flow conditions is shown in Fig. 1.

The objectives of our experiments were to study the effects of flow conditions and solidification parameters on feathery grains formation in an Al–4.5% Cu alloy. An experimental Al–Cu alloy with a chemical composition of

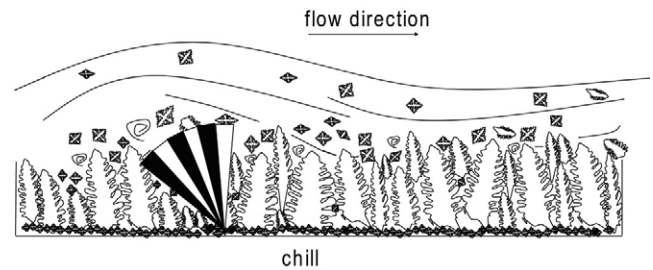


Fig. 1. Schematic illustration of solidification in a cavity under forced flow conditions.

4.47% Cu, 0.20% Si and 0.12% Fe was prepared using 99.95% pure aluminium and an Al–47.7% Cu master alloy. The samples were obtained in a velocity range of ~ 0.03 – 0.50 m s^{-1} and at melt temperatures in the liquid bath of 973, 993, 1013 and 1033 K, which corresponded to the initial superheats of 55, 75, 95 and 105 K, respectively.

Temperature was measured at different distances from the chill surface (1, 5, 10 mm) in the cavity and recorded by a computer equipped with a National Instruments data acquisition card and software.

After experiments, samples were sliced through the middle section in the longitudinal direction for the examination of macrostructure. After cutting in the longitudinal direction, samples were polished and etched with a 45 ml HCl, 15 ml HNO_3 , 15 ml HF and 25 ml H_2O solution (Tucker's reagent) for ~ 25 s in order to reveal the macrostructure of the whole section. Specimens for microstructure investigation were then taken in the central part of the slice at identical distances from the chill surface upwards to the final solidification surface and the microstructure was examined with an optical microscope (Neophot 30). Samples were also electro-oxidized at 20 V DC in a 3% HBF_4 water solution for ~ 60 s to reveal the grain structure, in particular feathery grains.

Samples for electron backscatter diffraction (EBSD) measurements were prepared by standard mechanical polishing up to $1 \mu\text{m}$, followed by electrolytic polishing on a Struers ElectroPol-5 (Electrolyte A2, $30 \text{ V} \pm 10 \text{ s}$) to remove any deformation associated with the mechanical polish. EBSD measurements were performed in an LEO438VP scanning electron microscope (SEM) with tungsten filament and equipped with an EBSD-system from EDAX-TSL (Digiview IV). During EBSD analyses, an accelerating voltage of 30 kV and a probe current of 3 nA were used, at a working distance of 19 mm. A step size of $15 \mu\text{m}$ was used for the EBSD mapping ($2580 \times 3550 \mu\text{m}$). The raw dataset was subjected to a standard grain dilatation clean up (grain dilatation 5° , minimum grain size 2). Results of the EBSD mapping are displayed as inverse pole figure map and pole figures.

3. Computer simulations

Computer simulations of solidification under forced flow conditions of an Al–4.5% Cu alloy were performed

with the commercial software Flow-3D™ (version 9.1; Flow-3D is a trademark of Flow Science Inc., Santa Fe, NM, USA). The code solves the Navier–Stokes equations for fluid flow using a finite-volume approach. A solidification drag model, segregation model and surface tension model are incorporated in the finite-volume iteration [12]. Equations are solved iteratively using a minimum time step of 10^{-9} s. The two-dimensional (2D) domain 140 mm long and 40 mm high is divided into 35,000 cells. A coupled computation of flow and thermal fields is applied using a uniform structured mesh.

In the simulations, the melt is flowing from the left to the right of the computational domain at constant velocity and melt temperature. Solidification starts as the flowing melt is brought into contact with the chill surface and then it proceeds under conditions of constant melt flow along solidification front. A series of calculations is performed in order to obtain the solidification behaviour under forced flow conditions and then compare them to flow patterns in the cavity without solidification [13]. Evolution of solid fraction and temperatures is calculated as a function of time and position in the sample. The chill is bound by ceramic material and all interfaces are impermeable to liquid alloy. The interface between the chill and the melt flow is no-slip. The free surface of the flowing melt is deformable, since the surface tension effect is considered.

The boundary conditions applied for different sides of computational domain are as follows: to model the cooling, the Dirichlet condition at the bottom of computational domain taken from experimental measurements is applied. The top of the domain is considered adiabatic. The boundary conditions at the inlet are the constant flow velocity and melt temperature. The outlet boundary is a zero heat flux. The heat transfer at the interfaces between ceramic material (before and after the chill) and melt flow is determined from a constant heat transfer coefficient of $100 \text{ W m}^{-2} \text{ K}^{-1}$; between the bronze chill and melt flow this coefficient is $1500 \text{ W m}^{-2} \text{ K}^{-1}$.

The thermophysical properties and phase diagram parameters of the model alloy (Al–4.5% Cu) used in the present work are described elsewhere [14].

The solidification model under forced flow conditions has been validated in previous work [13] against experimental temperature measurements obtained in various locations in the flowing melt and in the chill. The comparison of experimental and numerical data showed a reasonable agreement. The solidification parameters that are correlated further with structure parameters have been determined from calculated and measured temperature distributions.

4. Results

4.1. Growth of feathery grains

Analysis of the samples obtained during solidification in the cavity with applied forced flow along the solidification

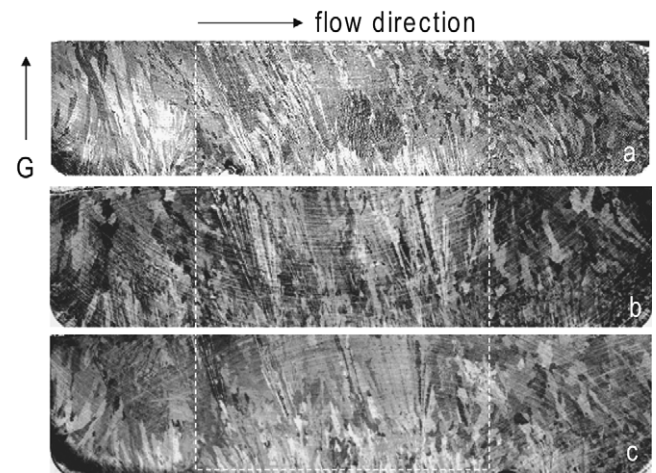


Fig. 2. Longitudinal macrostructure of samples obtained during solidification in the cavity under forced flow conditions at a bulk flow velocity of 0.03 m s^{-1} and initial melt temperatures of (a) 973 E, (b) 993 K and (c) 1013 K (G , thermal gradient); length of the sample is 100 mm.

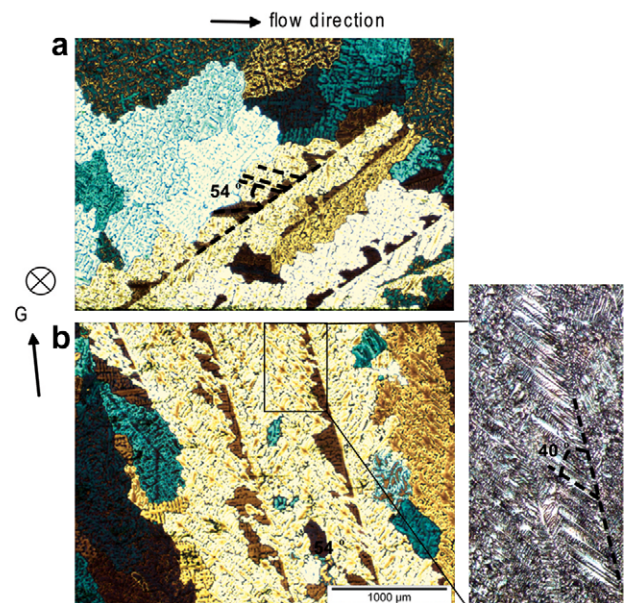


Fig. 3. Transverse (a) and longitudinal (b) structures with feathery grains.

front showed peculiar grain morphologies appearing under certain conditions [13]. The structure of the samples obtained at a low flow velocity of 0.03 m s^{-1} and at a high superheat of 55–95 K contained so-called feathery grains (Fig. 2). They mostly appeared in the central part (within the dashed frame in Fig. 2) of the sample, were deflected towards the incoming flow and started to grow either right at or 1–4 mm above the chill. Note that the thermal gradient (G) in Fig. 2 is slightly inclined towards the incoming flow. The fraction of feathery grains in the structure varied depending on the initial melt superheat. Moreover, the structure of each sample exhibited three types of morphology in different measures: pronounced columnar in the

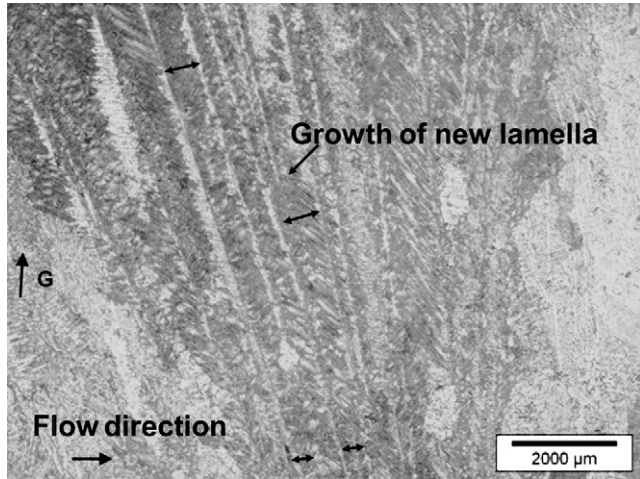


Fig. 4. Primary arm spacing in feathery grains depending on height from the chill surface.

upstream part; feathery in the central portion; and mixed columnar/equiaxed in the downstream corner of the cavity. All three morphologies can be clearly seen in Fig. 2a.

The electro-oxidized structure in Fig. 3 reveals typical feathery grains coinciding in transverse (a) and longitudinal (b) sections. Exhibiting different contrasts (originally in white and brown color), the grains consisted of parallel lamellae separated by wavy and straight boundaries. The equiaxed grains embedded in feathery crystals can be seen in the structure. The feathery grains were also bound by columnar grains whose growth was often suppressed. It is interesting that while the secondary arms grew at 54° from the twin plane (transverse section), they propagated at 40° from the primary trunk axis (longitudinal section; Fig. 3). It should be also pointed out that the secondary arms demonstrated pronounced growth in the direction towards the incoming flow.

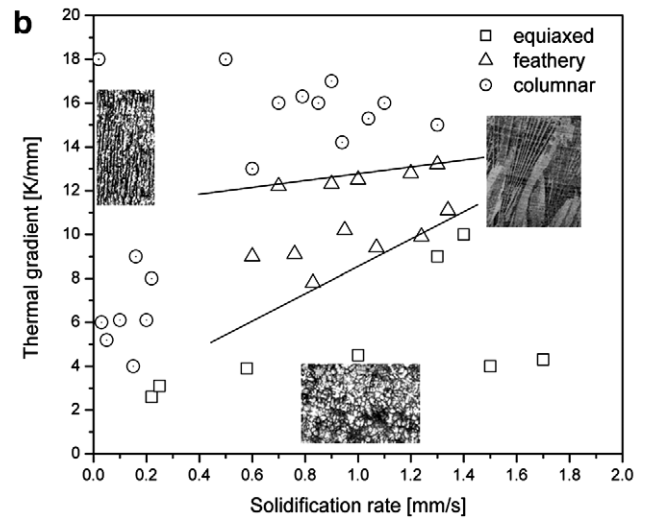
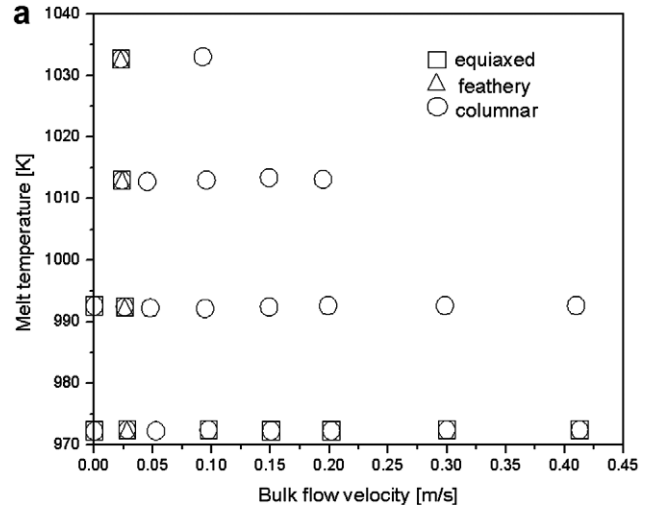


Fig. 6. Structural morphology depending on bulk flow velocity and initial superheat (a) and thermal gradient and solidification rate (b) in an Al–4.5% Cu alloy; a morphology type with a fraction >10% is considered to be present in the structure.

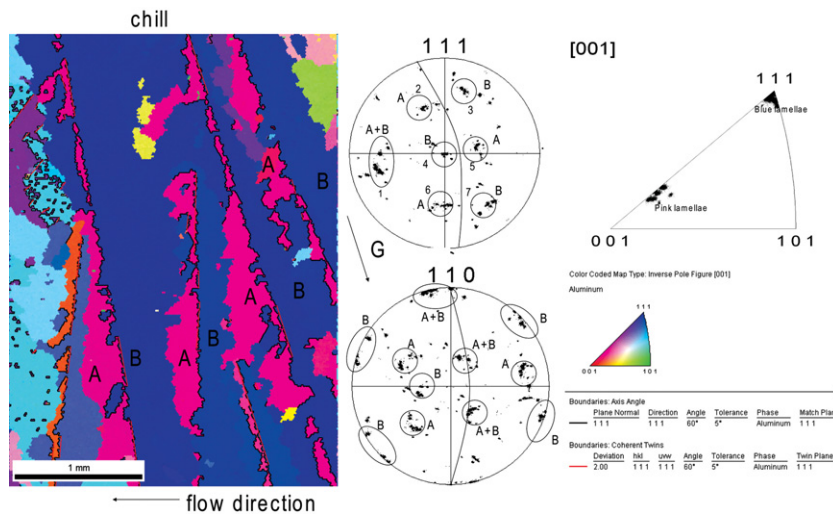


Fig. 5. Color-coded EBSD map (inverse pole figure) and corresponding $\langle 111 \rangle$ and $\langle 110 \rangle$ pole figures. For instance, in the $\langle 111 \rangle$ pole figure, cluster 1 contains both the blue and the pink lamellae; clusters 2, 5 and 6 belong solely to the pink lamellae and clusters 3, 4 and 7 belong solely to the blue lamellae.

Table 1

Solidification parameters for different superheats and identical bulk flow velocity of 0.03 m s^{-1} obtained from computer simulations and experimental measurements (\dot{T} , cooling rate; G , thermal gradient; V , solidification rate)

Superheat (K)	\dot{T} (K s^{-1})	G (K mm^{-1})	V (mm s^{-1})	G/V	Ref. in Fig. 2
55	1.76–3.8	3.8–8	0.22–1	3.8–36	<i>a</i>
75	0.8–11.7	9–13	0.06–1.3	7–216.6	<i>b</i>
95	0.18–14	10–18	0.01–1.4	7.1–1800	<i>c</i>

Additionally, it was also observed that the distance between primary trunks of feathery grains became larger as the distance from the chill increased. The feathery grains created a fan-like pattern. This trend was typical of all samples, independent of initial superheat (Fig. 4).

The crystallographic orientation of feathery grains was studied on a sample obtained under forced flow conditions at a bulk flow velocity of 0.03 m s^{-1} and initial superheat of 973 K. Fig. 5 gives an EBSD map obtained from the area close to the chill surface, showing the crystallographic orientation of the existing lamellae, with columnar and equiaxed grains also present in the structure. In order to reveal the crystallographic relationship between the lamellae, a $\langle 111 \rangle$ pole figure has been constructed from all measured points. Seven clusters of points can be clearly distinguished in the pole figure. These points correspond to the lamellae. The $\langle 111 \rangle$ zone with respect to the axis in point 1 will go through the three groups of clusters 2–3, 4–5 and 6–7. Whereas the $\langle 111 \rangle$ zone is tilted in the same direction as the lamellae in the EBSD map (direction of thermal gradient) and the $\langle 111 \rangle$ directions are symmetrically distributed with respect to the mentioned zone, it can be concluded that the A and B lamellae are in a twin relationship with each other. Thus, the feathery grains in this particular case are represented by coupled lamellae made of $\langle 111 \rangle$ trunks. The other directions on the pole figure most probably correspond to the columnar and equiaxed grains. Some misorientations existing within the lamellae can be also seen in Fig. 5.

4.2. Relationship between flow conditions, solidification parameters and structure morphology

Based on the analysis of the structure in the longitudinal section of the samples, the relationships between experiment conditions, such as bulk flow velocities and initial superheat with the structure morphology, have been obtained (Fig. 6). The influences of solidification parameters, such as thermal gradient and solidification rate have been additionally analyzed. The macrostructure of samples obtained under “no-flow” conditions consisted of either columnar or/and equiaxed grains depending on the cooling conditions and initial superheat. The applied forced flow ($<0.05 \text{ m s}^{-1}$), irrespective of initial superheat, resulted in the formation of a structure composed of equiaxed, feathery and columnar grains. Whilst accelerating the flow and increasing the superheat promoted columnar growth, the equiaxed structure can be observed in samples obtained at the lowest superheat (Fig. 6a).

The morphology variation depending on solidification parameters such as thermal gradient and solidification rate is shown in Fig. 6b. The solid lines in this figure indicate the intermediate region between equiaxed and columnar growth and schematically designate the upper and lower limits of thermal gradient and solidification rate within which the feathery grains were developed. The feathery grains were favored to grow under thermal gradients in the range between 6 and 13 K mm^{-1} and solidification rates of $0.4\text{--}1.7 \text{ mm s}^{-1}$.

As an example, Table 1 demonstrates the solidification parameters obtained from computer simulations and experimental temperature measurements, which were responsible for the evolution of the structures shown in Fig. 2. Increase of the superheat led to an increase of the thermal gradient and a general decrease in solidification rate that promotes columnar growth.

5. Discussion

Experimental findings in combination with the results of computer simulations show that: (1) feathery grains develop under conditions of low bulk flow velocity in the present experimental scheme; (2) feathery grains consist of lamellae which are in a twin relationship with a $\{111\}$ twin plane and $\langle 111 \rangle$ growth direction; (3) primary and secondary arms demonstrate pronounced growth in the direction opposite to the incoming flow; and (4) solidification conditions altered by forced flow are crucial for feathery grain formation.

Previous work showed that the forced flow in the present experimental scheme influences the solidification parameters and the macro- and microstructure, promoting the change in morphology [13]. Current results demonstrate that the feathery grains are formed under conditions of slow bulk flow velocity and in a wide range of superheats. While the macrostructure of the sample obtained under “no-flow” conditions consisted of equiaxed and/or columnar grains, the slow forced flow resulted in the formation of “intermediate” morphology, well-known as feathery crystals (Figs. 2 and 6). Indeed, in Fig. 6b the transition between equiaxed and columnar grains is the zone where the feathery grains are formed. Interestingly, the structures shown in Fig. 2 represent the zones of different thermal (or solidification) conditions: decreasing the thermal gradient and increasing the solidification rate in the flow direction correspond to columnar, feathery and equiaxed (formed under forced flow) morphologies.

It has been showed more than once that columnar grains are deflected in the direction of incoming flow and that the growth of high-order arms is more pronounced on the upstream side of the primary trunk due to specific solutal and thermal gradients on upstream–downstream sides [15]. The same trend is observed for feathery grains: the primary trunks and secondary arms demonstrate pronounced growth in the direction opposite to forced flow (Figs. 3 and 4). The $\langle 110 \rangle$ pole figure (Fig. 5) indicates that the primary dendrite trunks grow in a $[01\bar{1}]$ direction with $\langle 110 \rangle$ -type secondary arms, which is in a good agreement with the extensive studies on growth mechanisms of feathery grains performed by Henry et al. [10].

A flow over a cavity with solidification and its effects on macro- and microstructure evolution has been discussed elsewhere [13]. The flow oscillations are influenced by free surface wave effects and by coupling of the oscillations of the shear layer over the cavity with the flow inside the cavity. Particularly, for incompressible flow the instabilities are caused by the interaction between the shear layer and the flow within the cavity [16]. Due to these instabilities, unsteady vertical structures are generated that travel along the cavity producing high fluctuations in velocity and heat distribution. An instantaneous flow pattern developed in the cavity after initiation of the forced flow is shown in Fig. 7 for an inlet flow velocity of 0.03 m s^{-1} . A vortex can be observed in the cavity below the shear layer, traveling in the same direction as the initial flow. By the time the vortex reaches the downstream corner of the cavity it merges into the forced bulk flow. The flow pattern indicates the instabilities in the shear layer between forced and cavity flows [16]. Interestingly, the position of the vortex corresponds to the beginning of the zone (within the dashed frame in Fig. 2) where feathery grains are formed. It should be pointed out that there is some correlation between the flow pattern and the formation of feathery grains. Whilst the feathery crystals are mostly concentrated in the region close to the left side of the dashed frame in Fig. 2a for the initial superheat of 55 K, they are spread along the central part of the sample (within the dashed frame) for more superheated melts (75 and 95 K; Fig. 2b and c). Forced flow and high superheat slightly suppress the solidification rate (Table 1). As has been shown in Ref. [13], at low superheat and with fast solidification, the vortices tend to alter their structure from a circular to a longitudinal shape due to the geometrical aspect ratio of the cavity. At the same time, the velocity magnitudes in the vortex structure become smaller [13]. However, at higher superheats (75 and 95 K), the vortices appear and drift in the forced flow direction along the solid–liquid interface for a longer time, initiating stronger disturbances in the velocity field in this region and so producing stacking faults. This observation is in line with the findings of Henry et al. [6], who have demonstrated that the feathery grains appear in the region of the casting where the shear rate (or velocity field change) is maximum.

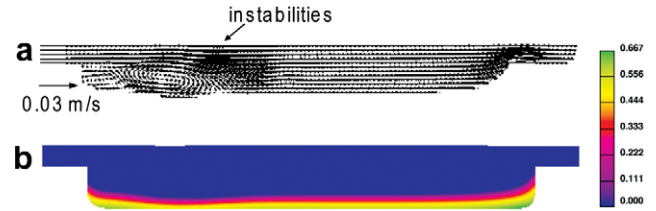


Fig. 7. Flow pattern (a) and solid fraction (b) for an inlet velocity of 0.03 m s^{-1} and an initial melt temperature of 973 K after 35 s.

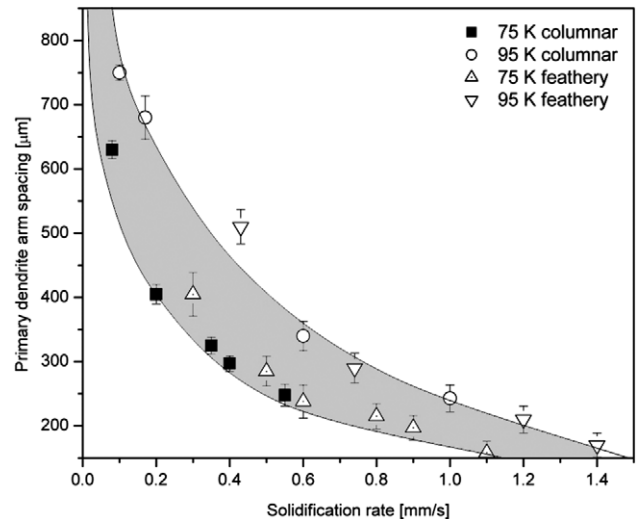


Fig. 8. Dependence of the primary dendrite arm spacing on solidification rate for regular columnar and feathery dendrites.

Our experimental results show that the spacing between primary trunks varies depending on the position in the cavity, e.g., with respect to the chill surface (Fig. 4). It has earlier been proposed [10] that the growth of twinned feathery grains occurs according to a competitive growth mechanism including branching similar to the growth of regular $\langle 100 \rangle$ dendrites. Fig. 8 demonstrates the dependence of the primary dendrite arm spacing on the solidification rate for regular columnar and for feathery dendrites in samples obtained at an identical bulk flow velocity and different superheats. In spite of the fact that two different heat regimes are characterized by different thermal gradients and their comparison is not entirely correct, it can be clearly seen that the dependence of primary dendrite arm spacing on solidification rate for feathery twins is aligned with the dependence for regular columnar dendrites. The peculiarity of feathery grain growth is the competition between branching (wavy boundary) and twinning (straight boundary). Thus, when the distance between the primary trunks becomes large enough, it gives rise to twinning (Figs. 4 and 8).

In summary, the onset of feathery growth seems to start under conditions of high thermal gradient along the solidification front when the slow flow is applied. The vortex

structure promoting high flow velocity fluctuations is found to play a determinative role in feathery twin development due most probably to a build up of shear stresses and stacking faults in the solidifying metal. Under favorable thermal gradients, once the twinned growth is initiated with the high solidification rate, it dominates over equiaxed and columnar growth. Under certain conditions of high thermal gradient and decreasing solidification rate, the feathery grain zone acquires a fan shape due to an increase in the distance between primary trunks (Figs. 2 and 5).

6. Conclusions

The solidified structure of an Al–4.5% Cu alloy obtained under different forced flow conditions was studied, with the focus on feathery grain formation. It has been shown that feathery growth is an intermediate case between equiaxed and columnar growth. The high velocity fluctuation promoted by a vortex structure affecting the solidification in the cavity under forced flow conditions results in the build-up of shear stresses and stacking faults in solidifying metal. This is believed to initiate the twinned feathery growth. Finally, it was demonstrated by the relationship between primary dendrite arm spacing and solidification rate that $\langle 110 \rangle$ feathery growth is similar to the growth of $\langle 100 \rangle$ regular dendrites with the competitive branching–twinning mechanisms. Macroscopic flow and thermal simulation give sufficient information for interpreting the observed structure patterns. However, microscopic structure modeling could be a subject of further investigation.

Acknowledgements

This work was carried out within the framework of the research program of the Netherlands Institute for Metals Research (www.nimr.nl), Project MC 4.02134. The authors thank J.J.H. van Etten, J.J. Jansen and J.P. Boomsma for practical assistance in performing the experiments and B. Doeve for sample preparation for EBSD measurements.

References

- [1] Cantor B, Vogel A. *J Cryst Growth* 1977;41:109.
- [2] Henry S, Minghetti T, Rappaz M. *Acta Mater* 1998;46:6431.
- [3] Shuvarikova EP. *Tsvet Met* 1987;1:80.
- [4] Muromachi S, Tada S, Tokizawa M, Anada H. *J Jpn Inst Light Met* 1980;30:545.
- [5] Anada H, Tada S, Koshimoto K, Hori S. *J Jpn Inst Light Met* 1991;41:497.
- [6] Henry S, Gruen GU, Rappaz M. *Metall Mater Trans A* 2004;35:2495.
- [7] Gullman LO, Johansson L. *AIME* 1972;345:437.
- [8] Matsuda F, Nakata K, Miyanaga Y, Kayano T, Tsukamoto K. *JWRI* 1978;7:33.
- [9] Henry S, Jarry P, Jouneau PH, Rappaz M. *Metall Mater Trans A* 1997;28:207.
- [10] Henry S, Jarry P, Rappaz M. *Metall Mater Trans A* 1998;29:2807.
- [11] Turchin AN, Eskin DG, Katgerman L. *Mater Sci Eng A* 2005;413–414:98.
- [12] Flow-3D. User's Manual V.9.1.
- [13] Turchin AN, Eskin DG, Katgerman L. *Metall Mater Trans A* 2007; in press.
- [14] Vreeman CJ, Incropera FP. *Int J Heat Mass Trans* 2000;43:687.
- [15] Okamoto T, Kishitake K, Bessho I. *J Cryst Growth* 1975;29:131.
- [16] Yao H, Cooper RK, Raghunathan S. *J Fluids Eng* 2004;126:919.